

SCIENTIFIC REPORTS



OPEN

Stress and temperature dependence of the avalanche dynamics during creep deformation of metallic glasses

Carlos Herrero-Gómez & Konrad Samwer

Received: 10 June 2016

Accepted: 25 August 2016

Published: 22 September 2016

The understanding of the mesoscopic origin of plasticity in metallic glasses remains still an open issue. At the microscopic level, Shear Transformation Zones (STZ), composed by dozens of atoms, have been identified as the basic unit of the deformation process. Macroscopically, metallic glasses perform either homogeneous or inhomogeneous flow depending on the experimental conditions. However, the emergence of macroscopic behavior resulting from STZ interactions is still an open issue and is of great interest. In the current work we present an approach to analyze the different interaction mechanisms of STZ's by studying the statistics of the avalanches produced by a metallic glass during tensile creep deformation. We identified a crossover between different regimes of avalanches, and we analyzed the dependence of such crossover on the experimental conditions, namely stress and temperature. We interpret such crossover as a transition from 3D random STZ activity to localized 2D nano-shear bands. The experimental time at which the crossover takes place seems to depend on the overall strain and strain rate in the sample

Amorphous materials have been known and used by mankind since ancient times¹, but several aspects of their physics remain nowadays elusive². Among those, the mesoscopic origin of plasticity in disordered materials in general, and Metallic Glasses (MG) in particular, is still debated³. MG's are one of the most promising amorphous materials for industry applications due to their outstanding mechanical⁴ magnetic⁵ and chemical properties⁶. They present extremely high elastic limit, but one of their main drawbacks is their brittle nature at room temperature^{7,8}. Unraveling the dependence of such macroscopic properties on the microscopic level is not only an open scientific topic, but is also crucial to foster industrial applications of MGs.

According to Argon's model, the unit of the deformation process in an amorphous solid is the so-called Shear Transformation Zone (STZ)^{9,10}. Such STZ's have been experimentally observed in colloidal glasses¹¹. Through an STZ process, the stress is relaxed by the collective shear of an ensemble of around 100 atoms, producing a long ranged stress Eshelby field with quadrupolar symmetry¹². For the production of a small shear band and his nucleation a cooperative activation of those Eshelby inclusions is needed¹³. Under uniaxial tensile conditions, such alignment should take place nearly at 45° along the highest stress component. Once the shear bands are formed, additional processes like cavity formation are important for the failure of the sample, via cracks¹⁴. Therefore, the cooperativity or interaction of the STZ's during the deformation turns out to be a key factor for the macroscopic behavior of the material.

In recent years, the plasticity of solid materials has been extensively studied in the framework of avalanche dynamics^{15–19}. Stress-drops in the plastic regime of stress-strain curves of MG's rods have been attributed to tuned criticality²⁰. Shear avalanches have also been reported in nano-indentation experiments²¹. Furthermore, there have been several attempts to study the units of the deformation process through different theoretical approaches^{22–24}. Apart from that, avalanche dynamics have been observed and studied in very different systems or situations, such as earthquakes²⁵, neuronal networks²⁶ or even some economy models²⁷. In all cases, avalanche dynamics are characterized by the jerky response of a system subjected to a continuous or constant excitation²⁸. This ragged response takes place without a characteristic scale, which is manifested in a power-law distribution

Physikalisches Institut, Georg-August Universität Göttingen, Friederich-Hund-Platz 1, 37077 Göttingen, Germany. Correspondence and requests for materials should be addressed to C.H.-G. (email: carlos.herrero@phys.uni-goettingen.de) or K.S. (email: ksamwer@gwdg.de)

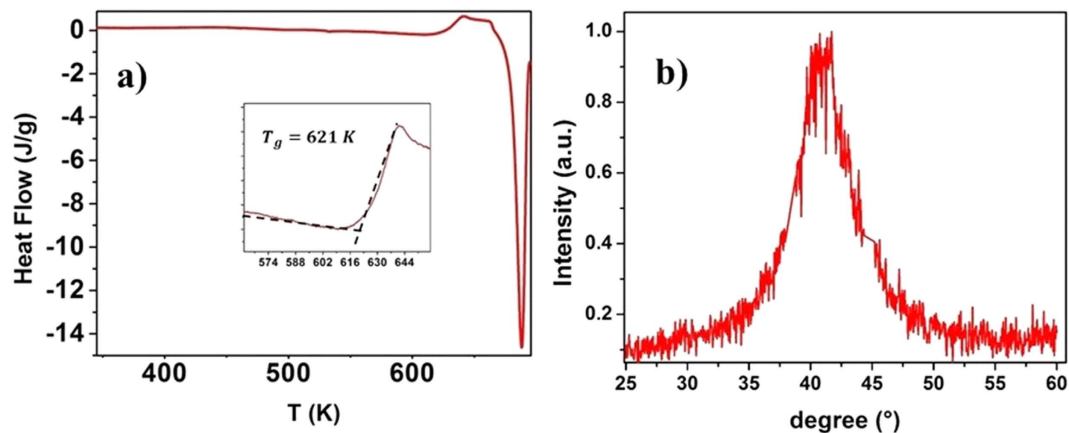


Figure 1. (a) DSC scan of a $\text{Pd}_{77.5}\text{Cu}_6\text{Si}_{16.5}$ Metallic glass sample. (b) and X-ray Diffraction pattern of a $\text{Pd}_{77.5}\text{Cu}_6\text{Si}_{16.5}$ sample.

of events sizes and durations. The exponents of those power-law distributions are believed to be universal and to depend on the type and dimensionality of the interactions present in the system²⁹.

In a previous work, a study of the avalanche dynamics in a metallic glass upon a creep experiment was reported³⁰. The main result was the finding of a crossover between two regimes of power-law scaling of the waiting time distribution. The waiting time was defined as the time required by the sample to deform 15 nm, which is the resolution limit of the device. That crossover took place between the exponents $\tau = -1.5$ and $\tau = -0.8$. Such crossover was interpreted as a change in the underlying mechanism of STZ's interaction. According to that interpretation, during the first regime the STZ's interact via stress-assisted randomly distributed avalanches (3D), and the second regime was attributed to an exhaustion of the first mechanism and its substitution by thermally activated (2D) correlated events.

The aim of the present work is to analyze the effect of the stress and temperature on the avalanche dynamics and the crossover between the two aforementioned regimes based on the waiting time analysis described in ref. 30 and to discuss the results based in the Potential Energy Landscape model (PEL)^{31–33}. According to that picture, the stress decreases the energy barriers of the PEL and enhances the thermal activation of STZ's which might assist a cooperative process¹⁰.

Here, we performed a set of creep experiments in $\text{Pd}_{77.5}\text{Cu}_6\text{Si}_{16.5}$ MG samples for a broad set of values of stress and temperature. In each of the experiments a freshly prepared 40 μm thick ribbon was subjected to a constant load and temperature during a week in order to provide reliable statistics. We find a significant variation of the crossover time with increasing temperature and stress. After the mechanical testing we made sure by X-ray measurements that the samples were not crystallized nor oxidized.

Experimental set-up

40 μm thick $\text{Pd}_{77.5}\text{Cu}_6\text{Si}_{16.5}$ ribbons were prepared by arc-melting and melt spinning, their amorphous structure was checked by X-Ray Diffraction using a D8000 XRD from Siemens and its glass temperature was measured by DSC as is depicted in Fig. 1.

The creep experiments were performed in a Dynamic Mechanical Analyzer (DMA-7) by Perkin Elmer, placed in a glove box in N_2 atmosphere to avoid oxidation at high temperatures. In those experiments the deformation as a function of time for a constant tensile stress and temperature was measured. Since the DMA lacks the resolution to resolve single microscopic elongation events (the spatial resolution is 15 nm), we analyzed the waiting times, which are defined as the elapsed time between two consecutive resolvable elongation jumps. The machine noise was filtered out using the same algorithm as described in ref. 30.

Experimental Results

Figure 2 shows a typical creep curve measured at $T = 593$ K and $\sigma = 20$ MPa. Although the elongation-time curve seems non linear but homogeneous on a global view, a closer look into the fine structure of the data shows a ragged and jerky shape, revealing a non-periodical distribution of jumps, which can be interpreted as a distribution of high and low strain rates.

A closer look to the waiting time distribution shows a crossover, where the scaling evolves with time from a power law with $\tau \sim -1.5$ in the early stages of the experiment to $\tau \sim -0.8$ later on (see Fig. 3b). Therefore, t_{cross} can be defined as an estimation of the experimental time in which the scaling of $P(\Delta t)$ crosses over from $P(\Delta t) \propto \Delta t^{-1.5}$ to $P(\Delta t) \propto \Delta t^{-0.8}$. We defined t_{cross} as the time that divides the data in two subsets ($t < t_{\text{cross}}$ and ($t > t_{\text{cross}}$) in such a way that minimizes the error of the fit of the experimental waiting time distributions of both subsets $P_1(\Delta t|t < t_{\text{cross}})$ and $P_2(\Delta t|t > t_{\text{cross}})$ and a perfect power law distribution $\tilde{P}_1 \sim \Delta t^{-1.5}$ and $\tilde{P}_2 \sim \Delta t^{-0.8}$ respectively. Figure 3a describes the crossover for the experiment corresponding to $T = 593$ K and $\sigma = 20$ MPa in the classical creep curve. Figure 3b shows the waiting time distributions $P_1(\Delta t|t < t_{\text{cross}})$ and $P_2(\Delta t|t > t_{\text{cross}})$ corresponding to the subsets of the data corresponding to before and after the crossover, together with the total

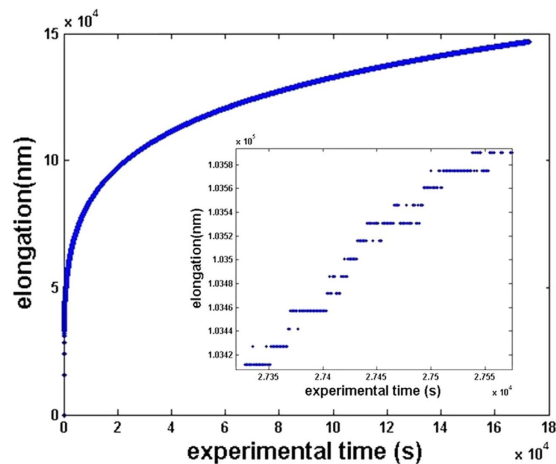


Figure 2. Creep measurement at $T = 320\text{ }^{\circ}\text{C}$ and $\sigma = 20\text{ MPa}$ and its fine structure (inset).

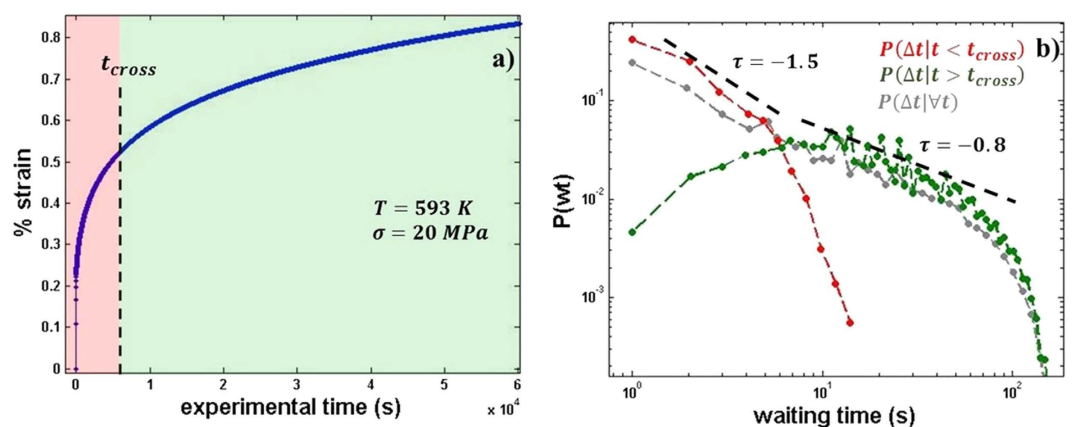


Figure 3. (a) Illustration of the crossover in the creep curve. (b) Waiting time distribution before the crossover: $P_1(\Delta t|t < t_{cross})$, after the crossover: $P_2(\Delta t|t > t_{cross})$ and for the whole experimental time $P(\Delta t|\forall t)$.

distribution of waiting times. In Fig. 3a no clear signature of crossover can be seen, but Fig. 3b illustrates that the crossover is a necessary condition to describe the data set in power laws of $P(\Delta t) \propto \Delta t^{-\tau}$.

To check if the crossover takes place under different experimental conditions, we performed a set of experiments for different values of stress and temperature in the range $\sigma = \{2-12\}$ and $\frac{T}{T_g} = \{0.85-0.94\}$. In each of the experiments a freshly prepared sample for the very same sample batch was subjected to a constant stress and temperature and the crossover time was estimated in the aforementioned described way. Figure 4 shows the stress-temperature map. Each square corresponds to a different creep measurement in which $P_1(\Delta t|t < t_{cross})$, $P_2(\Delta t|t > t_{cross})$ and the distribution of the whole set of waiting times is displayed. Finally, the background color represents the t_{cross} value. The power laws always start with a $\tau \sim -1.5$ dependence and shows later on a $\tau \sim -0.8$ dependency. Therefore t_{cross} is the estimation of the experimental time in which the $\tau \sim -0.8$ distribution is observed. It can be seen how t_{cross} increases both with temperature and stress.

Finally in order to analyze in detail the dependence of t_{cross} with the stress and temperature, we explored further the σ - T space by adding two sets of experiments to the results of Fig. 4. In the first one, the stress was kept constant ($\sigma = 12\text{ MPa}$) among the different experiments and the temperature was swept through the range $\frac{T}{T_g} = 0.67-0.98$. In the second run, the temperature is kept constant $\frac{T}{T_g} = 0.95$ and instead, the stress was swept in the range $\sigma = 2-35\text{ MPa}$, which corresponds to $\frac{\sigma}{E_g} = (0.05-0.6) \times 10^{-3}$, if we normalize by the Young modulus at that temperature. Figure 5 shows the dependence of t_{cross} with the stress and temperature.

Additionally, it can be observed in Fig. 3 that although the strain vs time curve and its derivative ($\dot{\epsilon}(t)$ vs t) are continuous functions, the average strain rate $\dot{\epsilon}(t)$ decreases dramatically with time at early experimental times, and eventually it reaches a steady state value. From the derivative of the macroscopic creep curves from the aforementioned experiments, we calculated the strain rate as a function of time $\dot{\epsilon}(t)$ vs t . We observed a decrease of the overall strain rate of one order of magnitude $\left(\frac{\dot{\epsilon}(t=0)}{\dot{\epsilon}(steady\ state)} \sim 10\right)$ for all our experiments. We also estimated from the

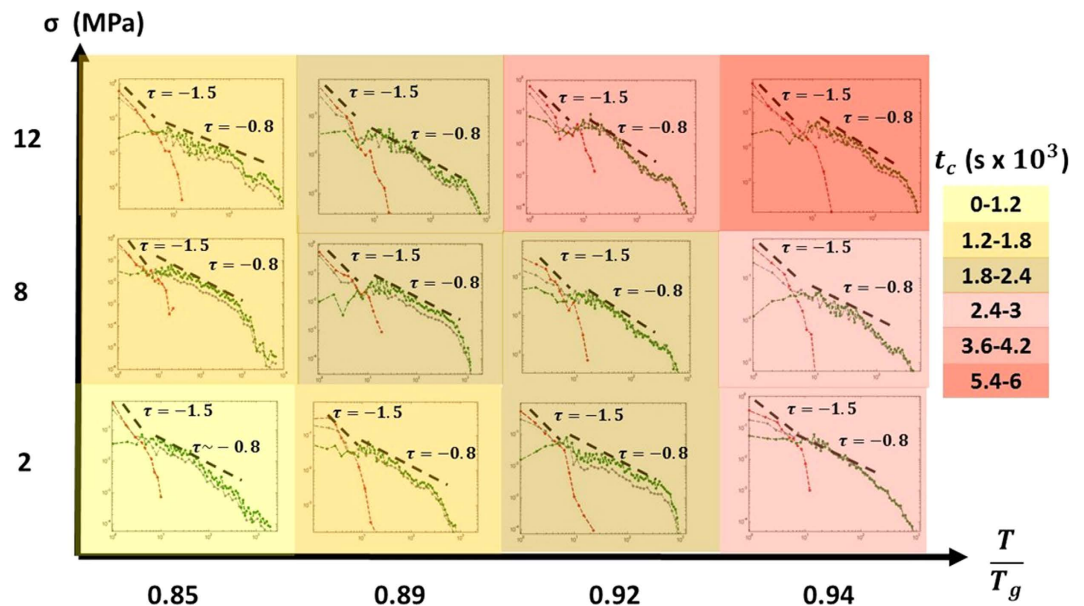


Figure 4. Stress-temperature map. Each square corresponds to a creep measurement under the corresponding $(\frac{T}{T_g}, \sigma)$ conditions. The background color represent the value of t_{cross} .

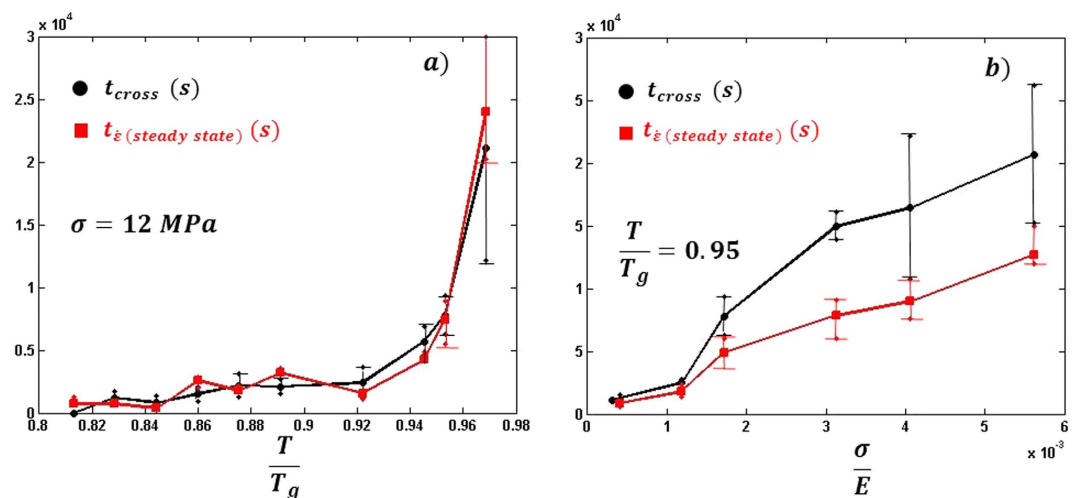


Figure 5. (a) Dependence of t_{cross} (black dots) and $t_{\dot{\epsilon}(steady\ state)}$ (red circles) with the temperature at a fixed stress. **(b)** Dependence of t_{cross} (black dots) and $t_{\dot{\epsilon}(steady\ state)}$ (red circles) with the stress at a fixed temperature. The errors bars indicate the range in which the fitted exponent take the values $\tau = 1.5 \pm 0.1$.

$\dot{\epsilon}(t)$ vs t curves the experimental time at which the sample reaches such steady state of lower strain rate $t_{\dot{\epsilon}(steady\ state)}$. Both quantities t_{cross} and $t_{\dot{\epsilon}(steady\ state)}$ show a clear correlation as can be seen in Fig. 5 in which both are displayed.

Figure 5a shows that at $\frac{T}{T_g} < 0.82$ no crossover can be seen within our experimental resolution. Therefore, if there is any crossover it must be faster than 1×10^3 s, but we are not able to observe any transition with good statistics. It also can be seen that as the temperature approaches the glass transition, t_{cross} increases rapidly. On the other hand Fig. 5b shows how t_{cross} increases in a more uniform fashion with the applied stress. When Fig. 5a is plotted in an Arrhenius-like fashion no clear $\frac{1}{T}$ dependence can be seen and the activation energy would be $E_A \sim 0.8$ eV, close to the one corresponding to diffusion jumps and suggests that the crossover is a combination of a thermal and mechanical process. Finally the clear correlation between t_{cross} and $t_{\dot{\epsilon}(steady\ state)}$ suggests a dependence of the crossover with the overall strain rate.

Discussion

In ref. 30 the existence of a crossover from two different scaling regimes of the waiting times during a creep experiment was reported. It was argued that such crossover can be related to a change on the microscopic deformation

mechanism in the MG. Such transition would be in agreement of the picture of a crossover from an uncorrelated 3-dimensional stress-driven plastic events regime (that would correspond to the $\tau_1 \sim -1.5$ regime) to a regime in which the main deformation mechanism is the thermal assisted collective nano-shear band activity in 2-dimensions ($\tau_2 \sim -0.8$).

Figure 4 points out that such crossover can be found under several experimental conditions. According to the model proposed in ref. 30 that means that in all that cases the deformation mechanism of the sample changes with time. It would start by a random activation of STZ's in the space, and once the STZ density reaches a critical value, the STZ's would cooperate forming 2-dimensional nano-shear bands.

The dependence of t_{cross} with temperature and stress is depicted in Fig. 5. Figure 5a shows how t_{cross} remains roughly constant or changes only slightly for low temperatures, and it increases dramatically as the temperature is increased approaching T_g . On the other hand, the data displayed in Fig. 5b show that t_{cross} increases in a roughly linear fashion with the applied stress. In both cases there is a clear correlation between the crossover time t_{cross} and the time at which the overall strain rate saturates to a constant value $t_{\dot{\epsilon}(steady\ state)}$.

It is known that macroscopic shear banding events are strongly affected by the strain rates. Those events tend to be intermittent at lower strain rates and successive at higher ones, leading to more pronounced serrations at low strain rates³⁴.

Such strain rate dependence supports the interpretation of a transition from 3D STZ's to 2D nano shear bands for the crossover in the creep experiments. The good correlation of t_{cross} with $t_{\dot{\epsilon}(steady\ state)}$ suggests that the system requires a constant strain rate to perform 2D nano shear bands.

The results depicted in Fig. 5 can also be interpreted in terms of the Eshelby correlations of the STZ's. A decrease of the correlations strength at temperatures approaching T_g is expected due it randomizing effect and the acceleration of the relaxations. Such an effect is in agreement with the results shown in Fig. 5a. On the other hand the delay of the crossover at high stresses can also be addressed by the effect of the higher overall strain in the sample. Such increase of strain according to the uniaxial stress applied to the sample follows the stress under approximately 45° inside the sample. Therefore, it reduces the interaction among STZ's via their Eshelby's stress field, which decreases with a $\frac{1}{r^2}$ dependence. That implies that the onset of cooperativity among the STZ's could be significantly delayed with a linear stress dependence and therefore the crossover might take place at a later time as the stress is increased while keeping the temperature constant.

Methods

Sample preparation. The glassy $Pd_{77.5}Cu_6Si_{16.5}$ samples were prepared using arc-melting and melt-spinning method. The thickness of the samples are roughly 40 μm . The glass transition was measured by DSC and was found at 621 K.

DMA creep measurements. The experiments were performed on samples mounted in metallic holders and clamped in a PerkinElmer DMA 7.A minimum pre-estress of 1.5 MPa was applied to keep the samples straight and stable during the heating process. The creep experiment was not started until the temperature reached a stable value. Once the temperature was stable a constant stress was applied and the elongation as a function of time was measured. The DMA7 was placed in a glove box in N_2 atmosphere to avoid oxidation of the samples.

Waiting time analysis and crossover. The machine noise was filtered using the same procedure as proposed in ref. 30. The error bars of the estimated crossover time in Fig. 5 correspond to the interval of time in which $\tau_1 = 1.5 \pm 0.1$.

References

- Grose, D. F. Early ancient glass: core-formed, rod-formed, and cast vessels and objects from the late Bronze Age to the early Roman Empire, 1600 B.C. to A.D. 50. New York: Hudson Hills Press in association with the Toledo Museum of Art. (1989).
- Debenedetti, P. G. & Stillinger, F. H. Supercooled liquids and the glass transition. *Nature* **410**, 259–267 (2001).
- Hufnagel, T. C., Schuh, C. A. & Falk, M. L. Deformation of metallic glasses: Recent developments in theory, simulations, and experiments. *Acta Materialia* **109**, 375–393 (2016).
- Greer, A. L. Metallic Glasses. *Science* **267**, 1947–1953 (1995).
- Tiberto, P., Baricco, M., Olivetti, E. & Piccin, R. Magnetic Properties of Bulk metallic Glasses. *Adv. Eng. Mat.* **9**(6), 168–474 (2007).
- Wang, W. H. Bulk Metallic Glasses with functional Physical properties. *Adv mater* **21**, 4524–4544. (2009).
- Ashby, M. F. & Greer, A. L. Metallic glasses as structural materials. *Scripta Materiala* **54**, 321 (2006).
- Sarac, B. & Schroers, J. Designing tensile ductility in a metallic glass. *Nat. Comm.* **2158**, 4 (2013).
- Argon, A. S. Plastic deformation in metallic glasses. *Acta Metall.* **27**, 47–58 (1979).
- Johnson, W. L. & Samwer, K. Universal criterion for plastic yielding of Metallic Glasses with a $\left(\frac{T}{T_g}\right)^{\frac{2}{3}}$ Temperature Dependence. *Phys Rev Lett* **95**, 195501 (2005).
- Schall, P. *et al.* Structural rearrangements that govern flow in colloidal glasses. *Science* **318**, 21(2007).
- Eshelby, J. D. The determination of the elastic field of an ellipsoidal inclusion, and related problems. *Proc. R. Soc. London Ser. A: Math. Phys. Eng. Sci.* **241**, 376–396 (1957).
- Dasgupta, R., George, H., Hentschel, E. & Procaccia, I. Microscopic Mechanism of Shear Bands in Amorphous Solids. *Phys. Rev. Lett.* **109**, 255502 (2012).
- Homer, E. R., Rodney, D. & Schuh, C. A. Kinetic monte carlo study of activated states and correlated shear-transformation zone activity during the deformation of an amorphous metal. *Phys. Rev. B* **81**, 064204 (2010).
- Dahmen, K. A., Ben-Zion, Y. & Uhl, J. T. Micromechanical Model for Deformation in Solids with universal predictions for Stress-Strain Curves and Slip Avalanches. *Phys. Rev. Lett* **102**, 175501 (2009).
- Budrikis, Z. & Zapperi, S. Avalanche localization and crossover scaling in amorphous plasticity. *Phys. Rev. E* **88**, 062403 (2013).
- Karmakar, S., Lerner, E. & Procaccia, I. Statistical physics of the yielding transition in amorphous solids. *J Phys. Rev. E* **82**, 055103 (2010).
- Maloney, C. E. & Lemaitre, A. Amorphous systems in athermal, quasistatic shear A. *Phys. Rev. E* **74**, 016118 (2006).

19. Lematre, A. & Caroli, C. Rate-dependent avalanche size in athermally sheared amorphous solids *C. Phys. Rev. Lett.* **103**, 065501 (2009).
20. Antonaglia, J. *et al.* Tuned Critical Avalanche Scaling in Bulk Metallic Glasses. *Scientific Reports* **4**, 4382 (2014).
21. Bian, X. L. *et al.* Shear avalanches in metallic glasses under nanoindentation: Deformation units and rate dependent strain burst cut-off. *Appl. Phys. Lett.* **103**, 101907 (2013).
22. Karmakar, S., Lerner, E., Procaccia, I. & Zylberg, J. Statistical physics of elastoplastic steady states in amorphous solids: finite temperatures and strain rate *Phys. Rev. E* **82**, 031301 (2010).
23. Lerner, E. & Procaccia, I. Locality and nonlocality in elastoplastic responses of amorphous solids. *Phys. Rev. E* **79**, 066109 (2009).
24. Dahmen, K. A., Ben-Zion, Y. & Uhl, J. T. A simple analytic theory for the statistics of avalanches in sheared granular materials. *Nat. Phys.* **7**, 554–557 (2011).
25. Sornette, A. & Sornette, D. *Self-Organized Criticality of Earthquakes*. *Europhys. Lett* **9**, 3 (1989).
26. Lombardi, F. *et al.* Balance between Excitation and Inhibition Controls the Temporal Organization of Neuronal Avalanches. *Phys. Rev. Lett.* **108**, 228703 (2012).
27. Bartolozzi, M., Leinweber, D. B. & Thomas, A. W. Scale free avalanche dynamics in the stock market. *Phys. A.* **1**, 370, 132–139 (2006).
28. Sethna, J. P., Dahmen, K. A. & Myers, C. R. Crackling Noise. *Nature* **410**, 242–250 (2001).
29. Kuntz, M. C. & Sethna, J. P. Noise in disordered systems: The power spectrum and dynamic exponents in avalanche models. *Phys. Rev. B* **62**, 17 (2000).
30. Krisponeit, J. O. *et al.* Crossover from random three-dimensional avalanches to correlated nano shear bands in metallic glasses. *Nat. Comm* **4616** (2014).
31. Stillinger, F. H. & Weber, T. A. Hidden structure in liquids. *Phys. Rev. A* **25**, 978–989 (1982).
32. Malandro, D. L. & Lacks, D. J. Relationships of shear-induced changes in the potential energy landscape to the mechanical properties of ductile glasses. *J. Chem. Phys.* **110**, 4593–4601 (1999).
33. Harmon, J. S., Demetriou, M. D., Johnson, W. L. & Samwer, K. Anelastic to plastic transition in metallic glass-forming liquids. *Phys. Rev. Lett.* **99**, 135502 (2007).
34. Jiang, W. H. *et al.* Rate dependence of shear banding and serrated flows in a bulk metallic glass. *J. mater. Res.* **21**, No.9 (Sep 2006).

Acknowledgements

Authors want to thank U. Filippich for the sample preparation, J.O. Krisponeit for the development of the filtering method, and A. Lagogianni and B. Riechers for fruitful discussions. Financial support from the ITN-FP7 Marie Skłodowska-Curie program “VitriMetTech” N. 607080 is thankfully acknowledged.

Author Contributions

The measurements and data analysis were performed by C.H.-G. The interpretation of the data was done by C.H.-G. and K.S. who also supervised the research. The manuscript was wrote by C.H.-G. and K.S.

Additional Information

Competing financial interests: The authors declare no competing financial interests.

How to cite this article: Herrero-Gómez, C. and Samwer, K. Stress and temperature dependence of the avalanche dynamics during creep deformation of metallic glasses. *Sci. Rep.* **6**, 33503; doi: 10.1038/srep33503 (2016).



This work is licensed under a Creative Commons Attribution 4.0 International License. The images or other third party material in this article are included in the article’s Creative Commons license, unless indicated otherwise in the credit line; if the material is not included under the Creative Commons license, users will need to obtain permission from the license holder to reproduce the material. To view a copy of this license, visit <http://creativecommons.org/licenses/by/4.0/>

© The Author(s) 2016